

DISTRIBUTION OF SATELLITE GALAXIES IN HIGH REDSHIFT GROUPS

YOUANG WANG¹, CHANGBOM PARK², HO SEONG HWANG^{2,3}, XUELEI CHEN^{1,4}

Draft version October 24, 2018

ABSTRACT

We use galaxy groups at redshifts between 0.4 and 1.0 selected from the Great Observatories Origins Deep Survey (GOODS) to study the color-morphological properties of satellite galaxies, and investigate possible alignment between the distribution of the satellites and the orientation of their central galaxy. We confirm the bimodal color and morphological type distribution for satellite galaxies at this redshift range: the red and blue classes corresponds to the early and late morphological types respectively, and the early-type satellites are on average brighter than the late-type ones. Furthermore, there is a *morphological conformity* between the central and satellite galaxies: the fraction of early-type satellites in groups with an early-type central is higher than those with a late-type central galaxy. This effect is stronger at smaller separations from the central galaxy. We find a marginally significant signal of alignment between the major axis of the early-type central galaxy and its satellite system, while for the late-type centrals no significant alignment signal is found. We discuss the alignment signal in the context of shape evolution of groups.

Subject headings: dark matter – galaxies:halos – galaxies:structure – large-scale structure of universe
– methods : statistical

1. INTRODUCTION

In a cold dark-matter dominated universe, galaxies form within dark matter halos, and smaller halos form first, subsequently these may grow larger by accreting material and/or by merging with other halos. As a result, satellite galaxies are distributed within the dark matter halo of galaxy groups. Under the assumption that there is an unbiased distribution between the satellites and dark matter halo, the position of satellites can be used to determine the shape of the dark matter halo (Carter & Metcalfe 1980; Plionis et al. 1991; Fasano et al. 1993; Basilakos et al. 2000; Orlov et al. 2001; Plionis et al. 2004, 2006; Wang et al. 2008), and their kinematics could be used to estimate the halo mass (Zaritsky et al. 1993, 1997; McKay et al. 2002; Brainerd & Specian 2003; Katgert et al. 2004; van den Bosch et al. 2004; More et al. 2009). Or, if a spatial bias between the distribution of satellites and the underlying dark matter distribution is found, it would be a very important clue for us in the study of galaxy formation theory. The orientation of the satellites may also provide useful information on its formation and evolution process. High-resolution simulations have shown that subhalos tend to align with the major axis of their host halos (Knebe et al. 2004, 2008a,b; Libeskind et al. 2005; Wang et al. 2005; Zentner et al. 2005; Agustsson & Brainerd 2006; Kang et al. 2007; Faltenbacher et al. 2008; Knebe et al. 2010). Such effects could be examined with observations of satellites at different redshifts, to give a more comprehensive test of

the theoretical model.

The morphology and color of the satellites are directly related to formation history of the host group. It has long been known that galaxies exhibit a bimodality in color and morphology: morphologically early-type galaxies which are typically red and have little or no ongoing star formation, and morphologically late-type galaxies, typically blue with active star formation. It is well known that galaxy morphology depends on local density environment. Hubble & Humason (1931) found a larger population of ellipticals and lenticulars in galaxy clusters, and subsequent studies revealed the connection between galaxy morphology and environment in low redshift clusters of galaxies (Oemler 1974; Weinmann et al. 2006; Park & Hwang 2009), nearby galaxy pairs (Park et al. 2007, 2008), isolated galaxy-scale satellite systems (Ann et al. 2008), and galaxy pairs at high redshifts (Hwang & Park 2009). The color bimodality is noted by numerous studies at both low redshifts (Strateva et al. 2001; Blanton et al. 2003; Baldry et al. 2004; Kauffmann et al. 2004) and at high redshifts of $z \sim 1$ (Bell et al. 2004; Tanaka et al. 2005; Weiner et al. 2005; Conselice et al. 2007). However, investigation on the bimodality and morphology-radius relation for satellite galaxies in high redshift groups have so far been lacking, one of the aims of the present paper is to investigate these issues.

The alignment between satellite distribution and the orientation of the central galaxy has been studied extensively since the work of Holmberg (1969), who first found that satellites are located preferentially close to the minor axes of the central galaxy. Many subsequent works confirmed the presence of this “Holmberg effect” (Lynden-Bell 1976, 1982; Majewski 1994; Hartwick 1996; Zaritsky et al. 1997; Hartwick 2000; Kroupa et al. 2005; Koch & Grebel 2006; McConnachie & Irwin 2006; Metz et al. 2007), though not all reached the same conclusion (Hawley & Peebles 1975; Sharp et al. 1979; MacGillivray et al. 1982). One common limitation of

¹ Key Laboratory of Optical Astronomy, National Astronomical Observatories, Chinese Academy of Sciences, Beijing 100012, China; E-mail: wangyg@bao.ac.cn

² School of Physics, Korea Institute for Advanced Study, Dongdaemun-gu, Seoul 130-722, Korea

³ CEA Saclay/Service d’Astrophysique, F-91191 Gif-sur-Yvette, France

⁴ Center of High Energy Physics, Peking University, Beijing 100871, China

the early studies is that the sample used are relatively small. With the advent of the 2dF Galaxy Redshift Survey (2dFGRS) (Colless et al. 2001) and the Sloan Digital Sky Survey (SDSS) (York et al. 2000), much larger samples became available. Sales & Lambas (2004, 2009) found a tendency for the satellites to be located along the host major axes at the large-scale of $300 \text{ kpc} \lesssim r_p \lesssim 500 \text{ kpc}$ for a set of 1489 host galaxies with 3079 satellites from the 2dFGRS. This result is in a good agreement with similar studies carried out on the SDSS data (Brainerd 2005; Azzaro et al. 2007; Bailin et al. 2008; Agustsson & Brainerd 2010). Yang et al. (2006) and Wang et al. (2008) found a strong dependence of the alignment signal on the color of the central and satellite galaxies using groups in the SDSS Data Release 2 (DR2) and Data Release 4 (DR4) respectively. These studies found that the alignment signal is strongest between red central galaxies (hereafter ‘centrals’) and red satellites, while the satellites of blue centrals were consistent with being distributed isotropically. The alignment strength is also a function of the group mass, with stronger alignment signal in more massive groups. Other forms of alignment have also been studied, and some significant signals are detected. These include the alignment between neighboring clusters (Binggeli 1982; West 1989; Plionis 1994; Wang et al. 2009), between brightest cluster galaxies (BCGs) and their parent clusters (Carter & Metcalfe 1980; Binggeli 1982; Struble 1990; Niederste-Ostholt et al. 2010), between the orientation of satellite galaxies and the orientation of the cluster (Dekel 1985; Plionis et al. 2003), and between the orientation of satellite galaxies and the orientation of the BCG (Struble 1990; Faltenbacher et al. 2007).

For obvious reasons, most studies on satellite distribution have been limited to low redshifts, typically $z \lesssim 0.2$. Recently, Donoso et al. (2006) analysed a sample of relatively high redshift ($0.4 < z < 0.5$) Luminous Red Galaxies (LRGs) extracted from the SDSS DR4 and their surrounding structures to explore the presence of alignment effects. They confirmed that such alignment effect was also present at $z \sim 0.5$. Okumura et al. (2009) investigated the correlation between the orientation of giant ellipticals by measuring the intrinsic ellipticity correlation function of 83,773 SDSS LRGs at redshifts 0.16-0.47 and also found a positive alignment between pairs of the LRGs up to $30h^{-1}\text{Mpc}$ scales.

Deep galaxy redshift surveys such as the Great Observatories Origins Deep Survey (GOODS) (Giavalisco 2004) now enable us to study the satellite distribution at even higher redshifts. Another aim of our paper is to detect the alignment between the distribution of satellite galaxies and the orientation of their central galaxy at redshifts beyond the local universe by using GOODS data. We construct a group catalog using a Friends-of-Friends (FoF) method, then we study the alignment signals with this sample. Compared with the previous studies, the redshift range in our sample is $0.4 \leq z \leq 1.0$, which includes many high redshift groups ($z \sim 1$).

This paper is organized as follows. We describe the observational data used for this study in section 2, and the FoF group-finding method in section 3. In section 4, we present the properties of satellites in groups. The method to quantify the alignment signal is presented in section 5, and the results given in section 6. Section 7

summarize our results and discuss various related issues.

2. OBSERVATIONAL DATA SET

2.1. galaxy sample

The galaxy sample used here is selected by Hwang & Park (2009). Here we give a brief description of the data sample, and we refer the reader to Hwang & Park for more details.

We used a spectroscopic sample of galaxies in GOODS. GOODS is a deep multiwavelength survey covering two carefully selected regions including the Hubble Deep Field North (HDF-N, hereafter GOODS-North) and the Chandra Deep Field South (CDF-S, hereafter GOODS-South). Total observing area is approximately 300 arcmin^2 and each region was observed by NASA’s Great Observatories (*HST*, *Spitzer* and *Chandra*), ESA’s *XMM-Newton*, and several ground-based facilities. *HST* observations with Advanced Camera for Surveys (ACS) were conducted in four bands: *B* (F435W, 7200s), *V* (F606W, 5000s), *i* (F775W, 5000s), and *z* (F850LP, 10,660s). Among the sources in the ACS photometric catalog, Hwang & Park (2009) selected 4443 (2197 in GOODS-South, 2246 in GOODS-North) galaxies whose reliable redshifts are available. In our analysis, a volume-limited sample of 1332 galaxies with $M_B \leq -18.0$ and $0.4 \leq z \leq 1.0$ is used. The rest-frame *B*-band absolute magnitude M_B of galaxies is computed based on the ACS photometry with Galactic reddening correction (Schlegel et al. 1998) and K-corrections (Blanton & Roweis 2007). The evolution correction (an increase of $1.3M_B$ per unit redshift) was also applied to the rest-frame M_B (Faber et al. 2007).

2.2. Morphology Classification

Hwang & Park (2009) visually inspected the individual *Bviz* band images and *Bvi* color images of the galaxies in a volume-limited sample. The galaxy is divided into two morphological types: early types (E/S0) and late types (S/Irr). Early-type galaxies are those with little fluctuation in the surface brightness and color and possess good symmetry in morphology, while late-type galaxies show internal structures and/or variations in the color images.

3. GROUPS OF GALAXIES

A very important step in our investigation is to identify the galaxy groups. There are many different techniques to identify groups in the local and distant Universe (Yang et al. 2005; Koester et al. 2007; Li & Yee 2008; Wen et al. 2009). All of these methods have their own advantages and disadvantages, which we do not discuss here. We use the FoF method to find the groups. The FoF algorithm adopted here is that of Eke (2004) and Knobel et al. (2009). There are three adjustable parameters in the FoF algorithm: the linking length b , the maximum perpendicular linking length in physical coordinates L_{max} and the ratio between the linking length along and perpendicular to the line of sight R . If two galaxies i and j with comoving distances d_{ci} and d_{cj} satisfy the following two conditions, then they are assigned to the same group. The two conditions, respectively, are

$$\theta_{ij} \leq \frac{1}{2} \left(\frac{l_{\perp,i}}{d_{ci}} + \frac{l_{\perp,j}}{d_{cj}} \right) \quad (1)$$

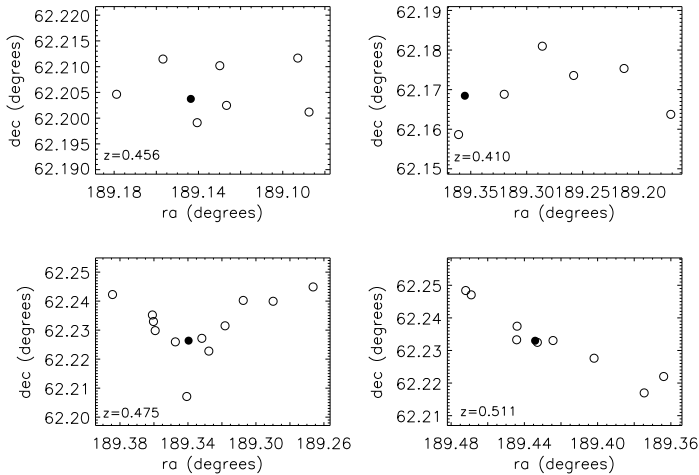


FIG. 1.— Four typical groups found by the FoF method. The three parameters b , L_{\max} and R are set $b = 0.11$, $L_{\max} = 0.45\text{Mpc}$, and $R = 13$, respectively. The filled and open circles represent the central and satellite galaxies, respectively.

and

$$|d_{ci} - d_{cj}| \leq \frac{l_{\parallel,i} + l_{\parallel,j}}{2}. \quad (2)$$

where θ_{ij} is the angular separation between galaxy i and j , and the two parameters l_{\perp} and l_{\parallel} are the comoving linking lengths perpendicular and parallel to the line of sight defined by

$$l_{\perp} = \min \left[L_{\max}(1+z), \frac{b}{\bar{n}^{1/3}} \right] \quad (3)$$

$$l_{\parallel} = R l_{\perp}, \quad (4)$$

where L_{\max} is the maximum perpendicular linking length in physical coordinates and \bar{n} is the mean density of galaxies. Since we have a volume-limited sample of galaxies, it is easy to obtain the value \bar{n} . For the typical value of three free parameters b , L_{\max} and R , we adopted them as listed in Table 1 of Knobel et al. (2009).

Figure 1 shows a few groups found by the FoF method. The three parameters b , L_{\max} and R are set as $b = 0.11$, $L_{\max} = 0.45\text{Mpc}$, and $R = 13$, respectively. In each group, the filled and open circles represent the central and satellite galaxies, respectively. The brightest galaxy in each group is defined as the central galaxy, and the rest are called its satellites. As shown in the top right panel of Figure 1, in some cases the “central galaxy” defined by this way is not actually located in the central region of groups. We call them the Deviation-Center-Group (DCG), and the other groups Located-Center-Group (LCG). The criterion for LCG is $d_a \leq \frac{1}{4}g_a$, where d_a is the angular distance between the brightest galaxy and the geometrical center of the group, and g_a is the angular size of the group. The half angular size of the group is defined as the angular separation between the geometrical center of the group and farthest member galaxy. In the determination of the alignment signal, only the LCGs are used. A total of 206 groups are found in our volume-limited sample.

In Figure 2, we show the redshift distribution of the groups in our sample. The distribution has a broad peak near $z \sim 0.7$.

4. PROPERTIES OF SATELLITES IN GROUPS

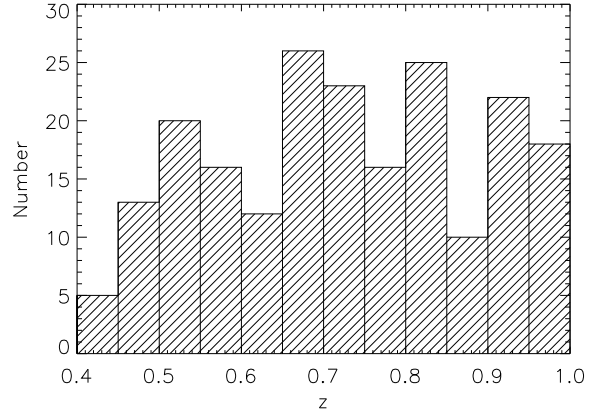


FIG. 2.— Redshift distribution of the groups.

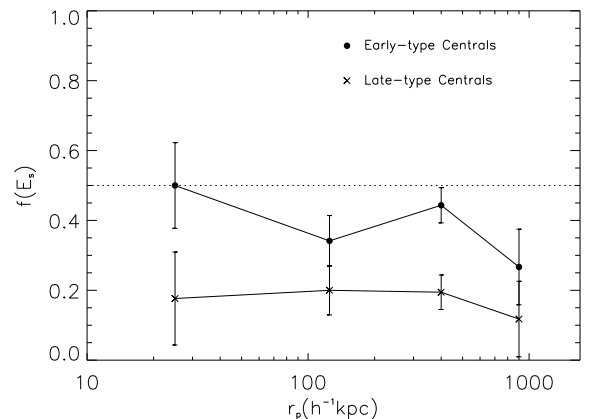


FIG. 3.— Early-type fraction of satellites galaxies as a function of projected distance from the central galaxy. The filled circles and crosses correspond to the early- and late-type central galaxy cases, respectively.

In Figure 3, we present the early-type fraction of satellites as a function of projected distance (r_p) from the central galaxy in groups. The filled circles and crosses are for the early- and late-type galaxy cases, respectively. The error bars represent 68% (1σ) confidence intervals, which are determined with the bootstrap resampling method. It is seen that the early-type fraction of satellites increases as satellites approach their early-type central galaxy. Also, the early-type fraction of satellites in groups with early-type centrals is higher than those with late-type centrals, which indicates that the satellite galaxies tend to have morphology similar to their centrals. Similar results have been obtained for galaxies in groups and clusters by Weinmann et al. (2006), for galaxy pairs in general environment by Park et al. (2007, 2008) in low redshift samples, and by Capak et al. (2007) and Hwang & Park (2009) in high redshift samples. In the group with a late-type central galaxy, the early-type fraction of satellites is nearly constant as the distance from the central galaxy changes.

In Figure 4, we show the rest frame B -band absolute magnitude M_B of the early- (filled circle) and late-type (cross) satellites as a function of the projected distance from the central galaxy. Two solid lines represent the

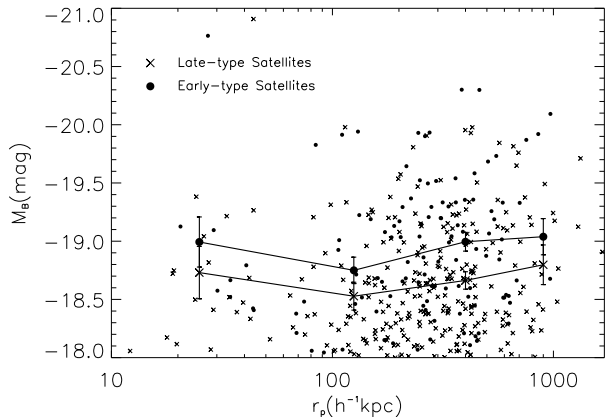


FIG. 4.— Rest frame B -band absolute magnitude M_B of the early- (filled circle) and late-type (cross) satellites as a function of the projected distance from the central galaxy. Two solid lines represent the median values.

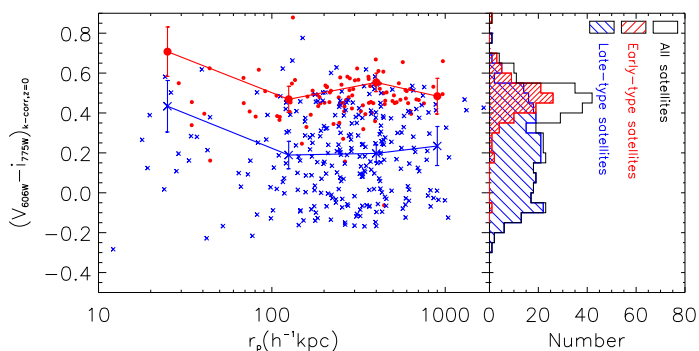


FIG. 5.— Color of the early- (filled circle) and late-type (cross) satellites as a function of the projected distance from the central galaxy (left panel). Two solid lines represent the median values. Color distributions for the satellite are shown by histograms in the right panel.

median values. The early-type satellites are on the average brighter than the late-type satellites.

In the left panel of Figure 5, we present the color of the early- (filled circle) and late-type (cross) satellites as a function of the projected distance from the central galaxy. V_{606W} and i_{775W} of galaxies are K-corrected (to $z=0$) magnitudes (Blanton & Roweis 2007). Two solid lines represent the median values. In the right panel of Figure 5, the distribution of color of satellites is shown. It can be clearly seen that the early- and late-type satellites occupy the red and blue bumps of the bimodal color distribution, respectively.

5. QUANTIFYING THE ALIGNMENT

In order to quantify the alignments of objects, we follow the method in Brainerd (2005) and compute the distribution functions of the alignment angles, $P(\theta)$, where θ is the angle between the major axis of the central group galaxy and the direction of a satellite relative to the centrals. The angle θ is constrained in the range $0^\circ \leq \theta \leq 90^\circ$, where $\theta = 0^\circ(90^\circ)$ suggests that the satellite lies along the major (minor) axis of the central

galaxy.

For a given set of the central and satellite galaxies, we first count the total number of central-satellite pairs, $N(\theta)$, for a number of bins in θ . Next, we construct 200 random samples in which we randomize the orientations of all centrals, and compute $\langle N_R(\theta) \rangle$, the average number of central-satellite pairs as function of θ . The random samples constructed this way suffer exactly the same selection effects as the real sample, so any significant difference between $N(\theta)$ and $N_R(\theta)$ reflects a genuine alignment between the orientations of the centrals and the distributions of their corresponding satellite galaxies.

Following Yang et al. (2006) and Wang et al. (2008), we introduce the distribution of normalized pair counts:

$$f_{\text{pairs}}(\theta) = \frac{N(\theta)}{\langle N_R(\theta) \rangle}. \quad (5)$$

In the absence of any alignment, $f_{\text{pairs}}(\theta) = 1$, while $f_{\text{pairs}}(\theta) > 1$ at small θ implies a satellite is preferentially aligned along the major axis of their central galaxy.

We quantify the fluctuation using $\sigma_R(\theta)/\langle N_R(\theta) \rangle$, where σ_R is the standard deviation of $N_R(\theta)$, and is estimated from the 200 random samples. In addition to this normalized pair count, we also compute the average angle $\langle \theta \rangle$. In the absence of any alignment $\langle \theta \rangle = 45^\circ$. If one finds $\langle \theta \rangle < 45^\circ$ ($\langle \theta \rangle > 45^\circ$), it means that the satellites are distributed along the major (minor) axis of the central galaxy.

6. ALIGNMENT MEASUREMENT

In order to study the alignment signal, the position angles of the central galaxies are required. We only use those groups with central galaxy axis ratio $b/a < 0.8$. For these galaxies, the isophotal position angle is well defined. Here a and b are the isophotal semi-major and minor axis lengths adopted from the i -band measurements in the HST/ACS photometric catalog, respectively. Finally, we have 168 central-satellite pairs in the detection of the alignment signal.

Figure 6 shows f_{pairs} for the selected central-satellite systems. There is a marginally significant signal of alignment between the orientation of the central galaxies and the distribution of the satellites. Satellite galaxies are distributed preferentially along the major axis of their central galaxy. This is also supported by the fact that $\langle \theta \rangle = 41.4 \pm 2.3$, which deviates from the case of no alignment (i.e. $\langle \theta \rangle = 45.0$) by 1.6σ . Moreover, a Kolmogorov-Smirnov (KS) test also suggests that an isotropic distribution of satellites in our sample is rejected with a confidence level higher than 90%. If we remove groups with $z > 0.6$ in our sample, then the alignment strength is changed from 1.6σ to 1.2σ .

In order to study how the alignment depends on the central galaxy properties, we divide our sample into early-type central and late-type central cases. Figure 7 shows the alignment signals $f_{\text{pairs}}(\theta)$ for the sample with early- (left panel) and late-type (right panel) central galaxies. As can be seen, systems with an early-type central galaxy shows 2σ alignment signal. A KS test finds that the sample with early-type centrals is not isotropic with confidence level higher than 99%. The distribution of $f_{\text{pairs}}(\theta)$ has an interesting shape, being greater at both $\theta \sim 0^\circ$ and $\theta \sim 90^\circ$ than at $\theta \sim 45^\circ$. This could

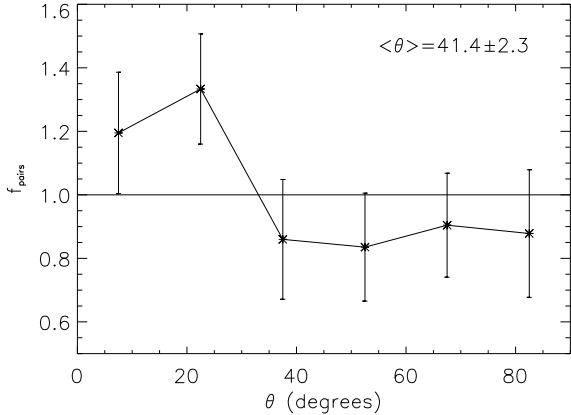


FIG. 6.— Normalized probability distribution, $f_{\text{pairs}}(\theta)$, of the angle θ between the major axis of the central galaxy and the distribution of satellites.

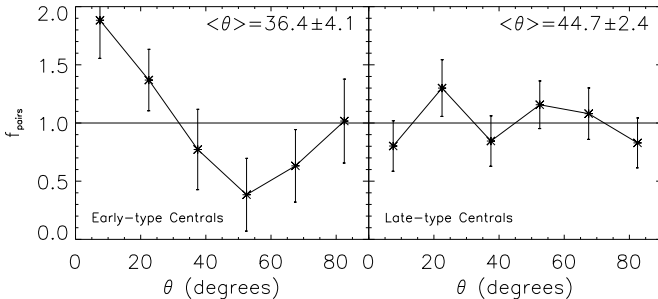


FIG. 7.— Same as Figure 6, but for different subsamples, divided by the morphological type of the central galaxy of the group.

perhaps be explained by the effect of infall from perpendicular filaments on forming galaxies (Brook et al. 2008). Systems with a late-type central galaxy, however, show no significant alignment. Compared with the alignment signal detected by Yang et al. (2006) ($\langle \theta \rangle = 42^\circ.2 \pm 0^\circ.3$) and Wang et al. (2008) ($\langle \theta \rangle = 42^\circ.46 \pm 0^\circ.12$) in low redshift groups, there is no significant difference (the confidence level for this tiny difference is below 0.5σ) between the alignment strength in high- z and local groups (for the total samples). In other words, no evolution of the alignment is seen within redshift $[0,1]$.

7. SUMMARY AND DISCUSSION

Using the FoF group finder, we create a high-redshift ($0.4 \leq z \leq 1.0$) group catalogue out of a spectroscopic sample of galaxies in the GOODS fields. We also identify the morphology of the satellite galaxies visually. The morphologically early- and late-type satellites occupy the red and blue bumps of the bimodal color distribution, respectively. We then study the early-type fraction, the magnitude-radius relation and the color-radius relations of the satellite galaxies in these groups. We find that the early-type fraction of satellites in early-host centrals is higher than those in late-type centrals. The early-type satellites are also on the average brighter than the late-

type satellites.

We measured the alignment between the distribution of satellites and the orientation of their central galaxy. We find a marginally significant alignment signal for the whole sample and for the subsample with early-type centrals. However, we do not find any alignment signal for the subsample with late-type centrals.

It is known that the group catalog strongly depends on the three adjustable parameters b , L_{max} and R in the FoF algorithm. In order to study how these parameters affect the measurement of the alignment signal, we have adopted five groups of parameter-sets as listed in Table 1 of Knobel et al. (2009) in identifying groups, and calculated alignment signals for each case. We find that the result of the alignment signal from the groups found by using the five different sets of group parameters are nearly the same. This indicates that our results on group central-satellites alignment is not sensitive to the choice of adjustable parameters in the FoF algorithm.

The measured alignment signal may be compared with numerical simulation results. Using N-body simulations, Jing & Suto (2002); Wang & Fan (2004) found that the non-sphericity of dark matter halos are greater at higher redshift, so we might expect a stronger alignment strength in the high-redshift groups. However, in our high redshift catalog we only find an alignment strength similar to the local groups.

There are several possibilities for this result. First, due to the limited number of pairs available, the sample variance is still large, and the detection is marginal. It is still difficult to draw conclusions from this observation. We have 168 central-satellite pairs in total and find a 1.6σ alignment signal. To check how the strength of alignment signal depends on the sample size, we use the SDSS DR4 data adopted in Wang et al. (2008) to make a test. The total number of central-satellite pairs in Wang et al. (2008) is 62212, and the alignment signal is 21σ ($\langle \theta \rangle = 42^\circ.46 \pm 0^\circ.12$). We randomly select 168×2 , 168×4 central-satellite pairs from this large sample, the corresponding alignment signal is detected at 2.4 , 2.5 and 3.9σ , respectively. If the same scaling is applicable to the high redshift sample, we need to increase our sample size by at least fourfold to reach a significant detection of about 3σ .

Second, we have assumed that stronger non-sphericity produce stronger alignments. To certain extent this should be true, as there would be no alignment signal when the distribution is spherical. However, at different redshifts the relation between non-sphericity and alignment may be different. For the same non-sphericity, the alignment might be weaker at higher redshifts due to some reason (e.g., less time for dynamical adjustment), thus partly compensated for effects of the stronger non-sphericity.

Finally, the predictions by Jing & Suto (2002); Wang & Fan (2004) were based on N-body simulations. Inclusion of baryon cooling effect may affect the shape of the halo (Kazantzidis et al. 2004; Debattista et al. 2008), and change the conclusions on the shape evolution of dark matter halos.

We may also compare the observational results of alignment strength at different redshifts in the literature. For the group in the range $0.01 \leq z \leq 0.2$ (Wang et al. 2008), the misalignment angle between the major axis of the

central galaxy and the projected major axis of the host halo follows a Gaussian distribution with zero mean and a dispersion of 23° . Using a sample at ($0.16 \leq z \leq 0.47$), Okumura et al. (2009) discovered that the misalignment angle between the central LRGs and their host halo also follows a Gaussian distribution with a zero mean, but the dispersion angle is $\sim 35^\circ$. If we extend this trend to samples at even higher redshifts, the misalignment angles should be larger. With such a trend, a weaker alignment signal is expected at higher redshifts.

In order to further improve our understanding of the spatial distribution of satellites in high redshift groups, we need a large sample. Some ongoing surveys, such as the Canada-France-Hawaii Telescope (CFHT) Legacy Survey, may extend the sample size significantly, and bring a definite answer to questions related to the distribution of satellites in the high redshift groups.

ACKNOWLEDGMENTS

We sincerely thank the referee for the constructive and detailed comments and suggestions. This work has started during YGW's visit to KIAS, and he would like to express his gratitude to KIAS. CBP acknowledges the support of the Korea Science and Engineering Foundation (KOSEF) through the Astrophysical Research Center for the Structure and Evolution of the Cosmos (ARC-SEC). YGW acknowledges the support by the Young Researcher Grant of National Astronomical Observatories. XLC acknowledges the support by the NSFC Distinguished Young Scholar Grant No.10525314. YGW and XLC are also supported by the Ministry of Science and Technology under the 973 program (2007CB815401, 2010CB833004), and the CAS Knowledge Innovation Program (Grant No. KJXC3-SYW-N2).

REFERENCES

- Agustsson, I. & Brainerd, T. G. 2006, *ApJ*, 644, L25
 Agustsson, I. & Brainerd, T. G. 2010, *ApJ*, 709, 1321
 Ann, H. B., Park, C., & Choi, Y. 2008, *MNRAS*, 389, 86
 Azzaro, M., Patiri, S. G., Prada, F., & Zentner, A. R. 2007, *MNRAS*, 376, L43
 Bailin, J., Power, C., Norberg, P., Zaritsky, D., & Gibson, B. K. 2008, *MNRAS*, 390, 1133
 Baldry, I. K., Glazebrook, K., Brinkmann, J., et al. 2004, *ApJ*, 600, 681
 Basilakos, S., Plionis, M., & Maddox, S. J. 2000, *MNRAS*, 316, 779
 Bell, E. F., Wolf, C., Meisenheimer, K., et al. 2004, *ApJ*, 608, 752
 Binggeli, B. 1982, *A&A*, 107, 338
 Blanton, M. R., Hogg, D. W., Bahcall, N. A., et al. 2003, *ApJ*, 594, 186
 Blanton, M. R. & Roweis, S. 2007, *AJ*, 133, 734
 Brainerd, T. G. 2005, *ApJ*, 628, L101
 Brainerd, T. G. & Specian, M. A. 2003, *ApJ*, 593, L7
 Brook, C. B., Governato, F., Quinn, T., et al. 2008, *ApJ*, 689, 678
 Capak, P., Abraham, R. G., Ellis, R. S., et al. 2007, *ApJS*, 172, 284
 Carter, D. & Metcalfe, N. 1980, *MNRAS*, 191, 325
 Colless, M., Dalton, G., Maddox, S., et al. 2001, *MNRAS*, 328, 1039
 Conselice, C. J., Bundy, K., Trujillo, I., et al. 2007, *MNRAS*, 381, 962
 Debattista, V. P., Moore, B., Quinn, T., et al. 2008, *ApJ*, 681, 1076
 Dekel, A. 1985, *ApJ*, 298, 461
 Donoso, E., O'Mill, A., & Lambas, D. G. 2006, *MNRAS*, 369, 479
 Eke, V. R., et al. 2004, *MNRAS*, 348, 866
 Faber, S. M., Willmer, C. N. A., Wolf, C., et al. 2007, *ApJ*, 665, 265
 Faltenbacher, A., Jing, Y. P., Li, C., et al. 2008, *ApJ*, 675, 146
 Faltenbacher, A., Li, C., Mao, S., et al. 2007, *ApJ*, 662, L71
 Fasano, G., Pisani, A., Vio, R., & Girardi, M. 1993, *ApJ*, 416, 546
 Giavalisco, M., et al. 2004, *ApJ*, 600, L93
 Hartwick, F. D. A. 1996, in *Astronomical Society of the Pacific Conference Series, Vol. 92, Formation of the Galactic Halo...Inside and Out*, ed. H. L. Morrison & A. Sarajedini, 444–+
 Hartwick, F. D. A. 2000, *AJ*, 119, 2248
 Hawley, D. L. & Peebles, P. J. E. 1975, *AJ*, 80, 477
 Holmberg, E. 1969, *Ark.Astron.*, 5, 305
 Hubble, E. & Humason, M. L. 1931, *ApJ*, 74, 43
 Hwang, H. S. & Park, C. 2009, *ApJ*, 700, 791
 Jing, Y. P. & Suto, Y. 2002, *ApJ*, 574, 538
 Kang, X., van den Bosch, F. C., Yang, X., et al. 2007, *MNRAS*, 378, 1531
 Katgert, P., Biviano, A., & Mazure, A. 2004, *ApJ*, 600, 657
 Kauffmann, G., White, S. D. M., Heckman, T. M., et al. 2004, *MNRAS*, 353, 713
 Kazantzidis, S., Kravtsov, A. V., Zentner, A. R., et al. 2004, *ApJ*, 611, L73
 Knebe, A., Draganova, N., Power, C., et al. 2008a, *MNRAS*, 386, L52
 Knebe, A., Gill, S. P. D., Gibson, B. K., et al. 2004, *ApJ*, 603, 7
- Knebe, A., Libeskind, N. I., Knollmann, S. R., et al. 2010, *ArXiv e-prints*
 Knebe, A., Yahagi, H., Kase, H., Lewis, G., & Gibson, B. K. 2008b, *MNRAS*, 388, L34
 Knobel, C., Lilly, S. J., Iovino, A., et al. 2009, *ApJ*, 697, 1842
 Koch, A. & Grebel, E. K. 2006, *AJ*, 131, 1405
 Koester, B. P., McKay, T. A., Annis, J., et al. 2007, *ApJ*, 660, 239
 Kroupa, P., Theis, C., & Boily, C. M. 2005, *A&A*, 431, 517
 Li, I. H. & Yee, H. K. C. 2008, *AJ*, 135, 809
 Libeskind, N. I., Frenk, C. S., Cole, S., et al. 2005, *MNRAS*, 363, 146
 Lynden-Bell, D. 1976, *MNRAS*, 174, 695
 Lynden-Bell, D. 1982, *Observatory*, 102, 202
 MacGillivray, H. T., Dodd, R. J., McNally, B. V., & Corwin, Jr., H. G. 1982, *MNRAS*, 198, 605
 Majewski, S. R. 1994, *ApJ*, 431, L17
 McConnachie, A. W. & Irwin, M. J. 2006, *MNRAS*, 365, 902
 McKay, T. A., Sheldon, E. S., Johnston, D., et al. 2002, *ApJ*, 571, L85
 Metz, M., Kroupa, P., & Jerjen, H. 2007, *MNRAS*, 374, 1125
 More, S., van den Bosch, F. C., & Cacciato, M. 2009, *MNRAS*, 392, 917
 Niederste-Ostholt, M., Strauss, M. A., Dong, F., Koester, B. P., & McKay, T. A. 2010, *ArXiv e-prints*
 Oemler, A. J. 1974, *ApJ*, 194, 1
 Okumura, T., Jing, Y. P., & Li, C. 2009, *ApJ*, 694, 214
 Orlov, V. V., Petrova, A. V., & Tarantaev, V. G. 2001, *MNRAS*, 325, 133
 Park, C., Choi, Y., Vogeley, M. S., Gott, J. R. I., & Blanton, M. R. 2007, *ApJ*, 658, 898
 Park, C., Gott, J. R. I., & Choi, Y. 2008, *ApJ*, 674, 784
 Park, C. & Hwang, H. S. 2009, *ApJ*, 699, 1595
 Plionis, M. 1994, *ApJS*, 95, 401
 Plionis, M., Barrow, J. D., & Frenk, C. S. 1991, *MNRAS*, 249, 662
 Plionis, M., Basilakos, S., & Ragone-Figueroa, C. 2006, *ApJ*, 650, 770
 Plionis, M., Basilakos, S., & Tovmassian, H. M. 2004, *MNRAS*, 352, 1323
 Plionis, M., Benoist, C., Maurogordato, S., Ferrari, C., & Basilakos, S. 2003, *ApJ*, 594, 144
 Sales, L. & Lambas, D. G. 2004, *MNRAS*, 348, 1236
 Sales, L. & Lambas, D. G. 2009, *MNRAS*, 395, 1184
 Schlegel, D. J., Finkbeiner, D. P., & Davis, M. 1998, *ApJ*, 500, 525
 Sharp, N. A., Lin, D. N. C., & White, S. D. M. 1979, *MNRAS*, 187, 287
 Strateva, I., Ivezić, Ž., Knapp, G. R., et al. 2001, *AJ*, 122, 1861
 Struble, M. F. 1990, *AJ*, 99, 743
 Tanaka, M., Kodama, T., Arimoto, N., et al. 2005, *MNRAS*, 362, 268
 van den Bosch, F. C., Norberg, P., Mo, H. J., & Yang, X. 2004, *MNRAS*, 352, 1302
 Wang, H. Y., Jing, Y. P., Mao, S., & Kang, X. 2005, *MNRAS*, 364, 424
 Wang, Y., Park, C., Yang, X., Choi, Y.-Y., & Chen, X. 2009, *ApJ*, 703, 951

- Wang, Y., Yang, X., Mo, H. J., et al. 2008, MNRAS, 385, 1511
- Wang, Y.-G. & Fan, Z.-H. 2004, ApJ, 617, 847
- Weiner, B. J., Phillips, A. C., Faber, S. M., et al. 2005, ApJ, 620, 595
- Weinmann, S. M., van den Bosch, F. C., Yang, X., & Mo, H. J. 2006, MNRAS, 366, 2
- Wen, Z. L., Han, J. L., & Liu, F. S. 2009, ApJS, 183, 197
- West, M. J. 1989, ApJ, 344, 535
- Yang, X., Mo, H. J., van den Bosch, F. C., & Jing, Y. P. 2005, MNRAS, 356, 1293
- Yang, X., van den Bosch, F. C., Mo, H. J., et al. 2006, MNRAS, 369, 1293
- York, D. G., Adelman, J., Anderson, Jr., J. E., et al. 2000, AJ, 120, 1579
- Zaritsky, D., Smith, R., Frenk, C., & White, S. D. M. 1993, ApJ, 405, 464
- Zaritsky, D., Smith, R., Frenk, C., & White, S. D. M. 1997, ApJ, 478, 39
- Zentner, A. R., Kravtsov, A. V., Gnedin, O. Y., & Klypin, A. A. 2005, ApJ, 629, 219